J Sol-Gel Sci Technol (2012) 62:370–377
DOI 10.1007/s10971-012-2736-4

Biocompatible titania hydrogels with chemically triggered release of a photosensitive dye

Renata Rychtarikova · Gulaim A. Seisenbaeva · Gabriela Kuncova · Vadim G. Kessler

Received: 11 December 2011 / Accepted: 29 February 2012 / Published online: 16 March 2012

Abstract 5,10,15,20-Tetrakis(4-sulfonatophenyl)porphyrin was entrapped into biocompatible hydrogels formed by self-assembling micelles of the titanium dioxide prepared by hydrolysis of titanium ethoxide modified with triethanolamine (TEA). The materials were characterized by their optical and photosensitive properties. The immobilization led to changes of the absorption spectra of the dye and decreased its molar absorption coefficient. The TiO_2 matrix did not degrade the entrapped porphyrin upon u.v. irradiation. The formation of TEA–titanium(IV) chelates facilitated a controlled and triggered release of the immobilized dye from the hydrogels in lactate and citrate buffers. The released dye prolonged the sterility of citrate–phosphate buffer and its illumination with visible light inhibited growth of *Aspergillus niger*.

Keywords Sol–gel · Photosterilization · Immobilization · Biocompatible titanium dioxide · Porphyrin

1 Introduction

Photosensitizers are dyes (porphyrins, phenazines or phthalocyanines) containing chromophore (aromatic, heterocyclic) groups. Light absorption by the chromophores in aerobic atmosphere results in the formation of singlet oxygen ($^1O_2$) and other reactive oxygen species (ROS) that are efficient oxidizing agents for microorganism inhibition [1, 2]. The advantage of this method in environmental application [1, 3] is its simple experimental execution. In addition, the repeated exposure to the photodynamic process does not lead to formation of the resistance of the so treated microorganisms [4].

After cytotoxic effects of various free photosensitizers to numerous microorganisms [5] were established, their immobilization was studied to ensure their easier manipulation. Attention has also been paid to materials with a controlled and triggered release of the immobilized photosensitizer molecules. Unlike the firmly bound photosensitizers, the released photosensitizer molecule can readily approach cytoplasmatic membrane of infective microorganisms and induce stronger inhibition [1, 2]. Several materials with different mode of the dye release were applied to the photodynamic therapy of wound infections. According to need, alginate foams with curcumine disintegrate or remain as an intact gel layer as they are hydrated by the wound exudates [6]. Thermoresponsive gels containing entrapped porphyrin were prepared from (2-hydroxyethyl)methacrylate and its *N*-isopropylacrylamide copolymer. The release of the photosensitizer was controlled by the gel swelling that increased on heating the gel [7]. Bioadhesive patches with weakly bound 5-aminolevulinic acid and toluidine blue O have been proposed for treatment of candidosis and onychomycosis [8, 9]. Poly(vinyl alcohol) stabilized by borax served as a delivery system for cationic 5,10,15,20-tetrakis(*N*-methylpyridinium)porphyrin and methylene blue. These photosensitizer-loaded hydrogels should be capable of conforming to the shape and contours of a wound, but maintain structural integrity whilst in place [10].

For drug delivery and bioencapsulation, porous inorganic materials such as mesoporous silicas, hydroxyapatites,

R. Rychtarikova (✉) · G. Kuncova
Institute of Chemical Process Fundamentals AS CR, Rozvojova 135, 165 02 Praha 6, Suchdol, Czech Republic
e-mail: rychtarikova@icpf.cas.cz

G. A. Seisenbaeva · V. G. Kessler
Department of Chemistry, Swedish University of Agriculture Sciences, Box 7015, 75007 Uppsala, Sweden

tricalcium phosphates, aluminosilicates, mesoporous carbons, metal–organic frameworks, porous silicon, mesoporous organosilicates, calcium silicates, ceramic and carbon-based nanotubes, layered silicates and, last but not least, colloidal and hierarchically porous titanium oxide have recently attracted much attention. In these cases, bioactive molecules can be hosted within their pores without affecting their activity, ensuring their release in a controlled manner by zero-order kinetics [11–16].

Many metal oxides, in particular titanium(IV) dioxide, TiO_2, are highly biocompatible, at least in the absence of photochemical oxidation processes [17]. The development of titanium-based sol–gel materials suitable for bioencapsulation and controlled drug release has so far been impeded by the high reactivity of the metal–organic sol–gel precursors, titanium alkoxides, which required anhydrous media for preparing colloid solutions [18].

In this work, new biocompatible titanium materials that ensure chemically triggered release of entrapped 5,10,15,20-tetrakis(4-sulfonatophenyl)porphyrin are reported. These non-porous materials are formed by the TiO_2 micelles stabilized by chelate formation with the positively charged triethanolamine (TEA) and release the dye in a controlled manner in citrate and lactate buffers.

2 Experimental

2.1 Chemicals, microbiological media, and microorganism

Aspergillus niger 4054 strain was obtained from the Department of Biochemistry and Microbiology, Institute of Chemical Technology, Prague (Czech Republic).

Titanium(IV) ethoxide sols in ethanol containing different TiO_2 and triethanolamine (TEA) concentrations (Table 1) were prepared by the patented procedure [19]. Molar concentration of TEA, TiO_2, and HNO_3 (H^+) were calculated from the weight mass as $c_i = m_i/(M_i \times V)$, where M_i is the molar weight (149.188 g mol^{-1} for TEA, 79.866 g mol^{-1} for TiO_2, 63.013 g mol^{-1} for HNO_3) and m_i (in g) are TEA, TiO_2 and HNO_3 weight masses and V (in mL) corresponds to the sol volume. For HNO_3, $m_{H+} = \rho_{H+} \times V_{H+}$, where $\rho_{H+} = 1.512$ g cm^{-3} and V_{H+} in cm^3 are the density and the volume of HNO_3, respectively. Molar ratio of TEA to TiO_2 was defined as $\frac{n_{TEA}}{n_{TiO_2}} = \frac{M_{TiO_2}}{M_{TEA}} \times \frac{m_{TEA}}{m_{TiO_2}}$.

5,10,15,20-Tetrakis(4-sulfonatophenyl)porphyrin (TPPS) was purchased from Porphyrin Systems GbR (Germany). Potassium iodide, potassium phosphate dibasic, D-glucose, and sodium chloride were supplied by Lach-Ner (Czech Republic). Citric acid monohydrate, sodium phosphate dibasic dodecahydrate, potassium phosphate monobasic, and L-lactic acid (80 %) were obtained from Penta (Czech Republic). All chemicals were used in p.a. purity. Yeast extract was purchased from AppliChem (Germany), bacterial peptone from Oxoid (UK), and agar and ammonium molybdate from Sigma–Aldrich (Germany).

TPPS was dissolved in deionized water. The concentration (100 μmol L^{-1}) was checked by absorption spectrophotometry (the molar absorption coefficient of aqueous TPPS at 414 nm is $\varepsilon_A = 307$ L mmol^{-1} cm^{-1}).

Kinetics of TiO_2–TPPS dissolution was measured in citrate (100 mM)–phosphate (100 mmol L^{-1}; pH 6.0) and lactate (100 mmol L^{-1}; pH 5.5) buffers, respectively. The antimicrobial tests of the stability of the solution sterility were carried out in citrate (10 mmol L^{-1})–phosphate (20 mmol L^{-1}) buffer. Citrate–phosphate buffers were prepared by titration of Na_2HPO_4 with citric acid at 25 °C. The antimicrobial tests with *A. niger* were carried out with the use of the citrate–phosphate buffer prepared from aqueous Na_2HPO_4 (0.1 mol L^{-1}), bacterial peptone (2 g L^{-1}), and NaCl (9 g L^{-1}) titrated by citric acid (0.1 mol L^{-1}) to pH 6.0 at 25 °C. The lactate buffer was obtained by titration of L-lactic acid (100 mmol L^{-1}) with NaOH (5 mol L^{-1}).

Dilute saline solutions for microorganisms contained NaCl (8.5 g L^{-1}). YEPG medium was mixed from the yeast extract (10 g L^{-1}), bacterial peptone (10 g L^{-1}), and D-glucose (20 g L^{-1}). Agar (20 g L^{-1}) was added to obtain

Table 1 Composition of titanium(IV) ethoxide sols

Sample	Concentration (mol L^{-1})			Mol. ratio	
	TEA	TiO_2	H^+	TEA/TiO_2	H^+/TEA
TiO_2-1	0.904	1.531	0.0080	0.590	0.0084
TiO_2-2	0.870	1.470	0.0115	0.591	0.0132
TiO_2-3	0.840	1.414	0.0148	0.594	0.0176
TiO_2-4	0.902	1.344	0.0176	0.671	0.0195
TiO_2-5	0.750	0.950	0.0100	0.789	0.0133

the solid medium. The media and materials used in experiments with microorganisms were autoclaved (120 °C, 0.1 MPa, 20 min).

The iodometric agent was prepared from K_2HPO_4 (1 mol L^{-1}; 9.6 mL), KH_2PO_4 (1 mol L^{-1}; 40.4 mL), KI (19.9 g), and $(NH_4)_2MoO_4$ (2 mg), as reported [20]. The solution was filled up to 1,000-mL with deionized water in a volumetric flask that was wrapped up by a tinfoil for light-protection.

2.2 Preparation of porphyrin hydrogels and their scanning electron microscopy

TiO_2-1 and TiO_2-3 sols, respectively, were transferred with a syringe under argon atmosphere to a 500-μL Eppendorf tube and aqueous TPPS (100 μmol L^{-1}) was added. The mixtures were gently shaken and poured onto wafers. For the absorbance measurements, the hydrogels were prepared from 2-mL mixtures, while 500-μL mixtures were used in the other experiments. Plastic plates (3.5 cm^2), 10-mL beakers (for antimicrobial tests), and microscopic glasses (for $^1O_2$ luminescence measurement) were used as wafers. Gelation time at room temperature was 3–5 h.

SEM micrographs of TiO_2–TPPS hydrogels were imaged using a Hitachi TM-1000-μDeX 15 kV scanning electron microscope.

2.3 Compactness of hydrogels

The compactness of the hydrogels ensured by the balanced electrostatic interaction between positively charged TEA ligands adsorbed on the surfaces of TiO_2 micelles and the immobilized anionic TPPS was checked in deionized water. The samples of the hydrogels in distilled water (3 mL) were shaken on a Heidolph Unimax 1010 rotation shaker (Germany, 100 rpm) at room temperature for 1 h. Then, the washing water was transferred into a 10-mm quartz cuvette and its absorption spectrum was recorded with an HP 8452A spectrophotometer (USA; 2.2×10^{-3} a.u. sensitivity). For the hydrogels TiO_2-1 and TiO_2-3, no peaks corresponding to either the released TPPS ($\lambda_{max} = 414$ nm; $\varepsilon_A = 307$ L $mmol^{-1}$ cm^{-1} gives the detection limit of 7.2×10^{-8} mol L^{-1}) or TiO_2 (the absorption <350 nm) have been observed.

2.4 Fluorescence and absorbance

3D-fluorescence spectra of the TiO_2–TPPS hydrogels were collected with a Hitachi F-4500 spectrophotometer (Japan) at 25 °C with excitation/emission slits of 10/5 nm. Fluorescence intensities for the encapsulated TPPS were statistically evaluated at $\lambda_{EX}/\lambda_{EM} = 420/645$ nm.

Absorption spectra of the TiO_2–TPPS hydrogels were recorded with an HP 8452A spectrophotometer. Light-scattering was corrected with the Scatter correction function in the Advanced mode of UV/Vis ChemStation software (Agilent Technologies, Inc.) at 350–400 and 450–800 nm.

Thickness of the hydrogels was measured with a Carl Zeiss Primostar optical microscope (the upper and lower edges of the hydrogels were focused using a microscope microscrew). The absorption coefficient of immobilized TPPS was calculated from the equation $\varepsilon_H = \varepsilon_A \times \frac{A_H}{A_A} \times \frac{l_A}{l_H} \times k$, where A_A is the absorbance of aqueous TPPS at 414 nm, A_H is the absorbance of TPPS hydrogels at 420 nm, l_H is thicknesses of the hydrogels in cm, $k = 2$ is the vol. ratio of the hydrogels to aqueous TPPS (mL/mL), and l_A (in cm) is the optical length of the cuvette containing aqueous TPPS (in cm).

2.5 Illumination of immobilized TPPS with a halogen lamp and TiO_2 matrices by u.v. irradiation

The photosensitivity of TPPS immobilized in TiO_2 matrices was tested by illumination with a halogen lamp Osram 120V/300W (Germany), using the hydrogel samples placed on a piece of white paper. A dish (200 × 30) filled with water and centered between the lamp and the illuminated hydrogel served as an i.r. filter. Temperature gradient on hydrogel surfaces was 1 °C h^{-1} and the surface temperature did not exceed 30 °C.

The photosensitivity of TiO_2 matrices was tested by their irradiation with an A. Krüss Optronic u.v. lamp (Germany) placed 3 cm above the gel for 1 h. Then, their fluorescence spectra were collected with a Hitachi F-4500 spectrophotometer.

2.6 $^1O_2$ luminescence and iodometric method

The failure of the hydrogels to form internal $^1O_2$ was checked by their luminescence at 1,270 nm. The layer of TiO_2-1 on a glass was transferred into a cuvette and excited with a Lambda Physik FL 3002 dye laser ($\lambda_{exc} = 415$ nm, incident energy ca. 2 mJ $pulse^{-1}$). Time-dependent luminescence was detected with a home-made detector unit (interference filter, amplifier, Judson J16-8SP-R05M-HS Ge diode). The signal-to-noise ratio was improved by averaging 100–500 individual traces.

The potential production of surface ROS was tested by iodometric method [12] based on the following oxidation:

$$2\,I^- \xrightarrow{-2e} I_2$$

$$I_2 + I^- \rightarrow I_3^-$$

The iodometric agent was poured over the hydrogels and the mixture was shaken at 100 rpm with a Heidolph

Unimax 1010 rotation shaker and illuminated with a halogen lamp with the arrangement described in Sect. 2.5. In 0–30-min intervals, the samples of the iodide agent (100 μL) were transferred into a quartz cuvette (optical length of 10 mm, total volume 1 mL). Formation of the triiodide anion would be indicated by the appearance of the absorption band at 354 nm. The measurements showed that with the hydrogels under study (an HP 8452A spectrophotometer), the band has not been formed.

2.7 TPPS release to buffers

A total of 3 mL of lactate (100 mmol L^{-1}; pH 5.5) or citrate (100 mmol L^{-1})–phosphate (100 mmol L^{-1}; pH 6.0) buffer was poured onto the hydrogels and the mixture was shaken with a Heidolph Unimax 1010 rotation shaker (200 rpm). In 15-min intervals, the samples of the buffers (100 μL) were transferred into a quartz cuvette (10-mm optical length, total volume of 1 mL) and diluted with water in 1:9 vol. ratio. The intensity of the absorbance at 414 nm proportional to the amount of the TPPS released to the buffers was determined with an HP 8452A spectrophotometer.

Time-dependent TPPS release, $n_P = f(t)$, was smoothed in the Origin software by a sigmoid Bolzmann function $n_P = n_2 + \frac{n_1 - n_2}{1 + e^{\frac{t - t_c}{dt}}}$, where n_1/n_2 are the lower/upper limits of the sigmoid function corresponding to the initial/final molar amount of the released TPPS (in nmol), respectively, t_c is the time corresponding to the inflex point of the exponential part of the function at the molar amount of $(n_1 + n_2)/2$ (in h).

The rate of TPPS release and total dissolution time were calculated from $(n_2 - n_1)/4dt$ and $t_c + 2dt$, respectively.

2.8 Antimicrobial tests

Antimicrobial effect of the TPPS released from the hydrogels into citrate–phosphate buffer was tested by the two different procedures (Table 2).

The hydrogels placed at the bottom of the sterile 10-mL beakers were poured over by citrate (10 mmol L^{-1})–phosphate (20 mmol L^{-1}; pH 6.0; 5 mL) buffer and then the beakers were transferred on a piece of white paper under a light source. In the first test, the buffer was sterile and exposed to day light (500 lx) for 8 days, in the second experiment, the buffer was inoculated by *A. niger* 4054 strain and covered by a glass lid. Then the beakers were illuminated with a halogen lamp (10 klx) for 48 h with the arrangement described in Sect. 2.5. Positive control samples were treated with a mixture containing TPPS solution (100 μmol L^{-1}; 0.25 mL) and the buffer (5.25 mL). The buffer itself was used as a blank probe. Each sample was prepared in three replicates.

In fixed time intervals (Table 2), the suspensions (100 μL) were withdrawn and evaluated by the plate method (c.f.u. mL^{-1}) on YEPG agar (incubated at 30 °C for 48 h).

3 Results and discussion

3.1 Preparation of TiO_2–TPPS

Via process of the acid hydrolysis, titanium(IV) alkoxides dissolved in the parent alcohol and modified with triethanolamine (TEA) form the micelles that are stabilized by the positively charged TEA ligands adsorbed on their surface. The micelles were shown to possess a relatively small crystalline anatase core (2–3 nm) and an outer amorphous shell, as shown in Fig. 1 [16, 21].

Five titanium(IV) ethoxide sols were prepared with the use of different TEA and TiO_2 concentrations (Table 1). Formation of the hydrogels from the sols and aqueous TPPS (confirmed by the procedure described in Sect. 2.2) depended mainly on H^+/TEA mol. ratio in sols. While TiO_2-1 sol having the lowest H^+/TEA mol. ratio formed gel within less than 3 h, the TiO_2-3 sol gelation was complete after 5 h. As to the stability of the hydrogels, those having the high TEA/TiO_2 mol. ratios (TiO_2-4 and TiO_2-5) were unstable in water (Sect. 2.3). In the absence of either TPPS or TEA, a stable material was not formed.

The composites prepared from TiO_2-1 to TiO_2-3 sols containing very similar TEA/TiO_2 mol. ratios but the

Table 2 Conditions of antimicrobial tests

Differences	Experiment with sterile buffer	Experiment with *A. niger*
Citrate–phosphate buffer (pH 6.0)	5 mL, uncovered	4.5 + 0.5 mL of *A. niger* in YEPG broth, covered by a glass lid
Light source	Intensive day light (500 lx) by an open window	Halogen lamp (10 klx)
Buffer sampling	0, 1, 2, 5, and 8 days	0, 24, and 48 h
Petri dishes incubation	30 °C for 48 h	28 °C for 24 h

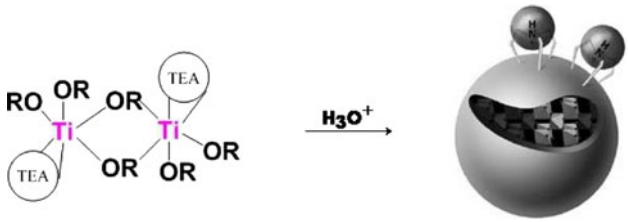

Fig. 1 Structure of a cluster (*left*) and a micelle (*right*) of titanium oxide formed by hydrolysis of an alkoxide precursor and supported by positively charged TEA self-assembling [19, 20]

highest difference in H^+/TEA mol. ratio were green–brown (Fig. 2) and are discussed hereinafter.

3.2 Absorbance, fluorescence, and photostability of TiO_2–TPPS hydrogels

The entrapment of TPPS into TiO_2-1 and TiO_2-3 hydrogels led to the decrease of the molar absorption coefficient of the Soret peak maximum from 307 (aqueous solution) to 281 (TiO_2-1) and 244 (TiO_2-3) L $mmol^{-1}$ cm^{-1}. As seen in Fig. 3, the interaction of the porphyrin with the matrix shifted the Soret band maxima from 414 to 420 nm as a consequence of the higher hydrophobicity and lower polarity of the matrix compared with water [22]. The strong electrostatic interactions between the anionic TPPS and the cationic TEA-stabilized matrix micelles were indicated by the deformation of the Q-bands. In all cases, TPPS was present in the monomer state [23]. The relatively huge peak observed with all hydrogels in u.v. region under 350 nm corresponded to TiO_2 absorption [24, 25].

The absorption spectra of the entrapped TPPS (Fig. 3) shew a doublet of the Soret peak maxima and a region of Q-peaks characteristic of non-protonized porphyrin [23]. The fluorescence spectra (Fig. 4) demonstrated that the porphyrin immobilized into TiO_2-1 and TiO_2-3 emitted at 645 nm with the average intensities of 2,009 and 2,246 a.u., respectively (Table 3).

Fig. 2 TiO_2-1 hydrogel with immobilized TPPS

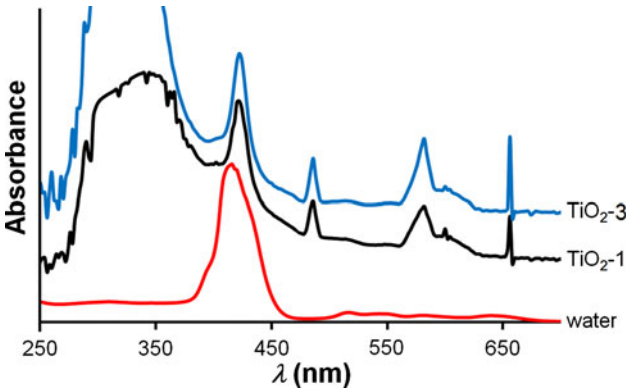

Fig. 3 Absorption spectra of TPPS in TiO_2 hydrogels and water (50 μmol L^{-1})

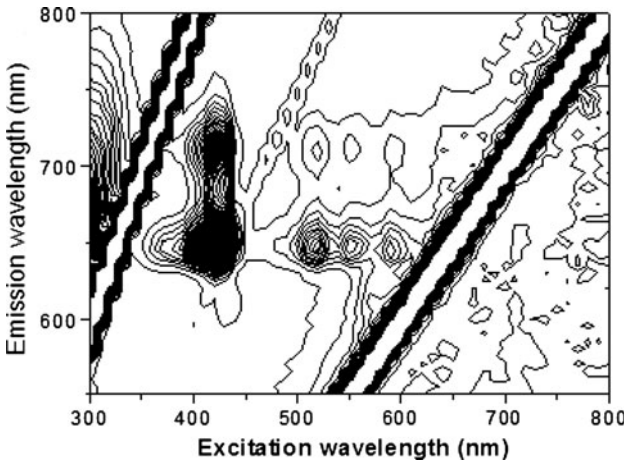

Fig. 4 3D-fluorescence spectrum of TiO_2-1. One contour corresponds to 100 a.u

Table 3 Fluorescence intensities of TiO_2–TPPS before and after u.v. irradiation at $\lambda_{EX}/\lambda_{EM}$ = 420/645 nm at 25 °C

Fluorescence intensity (a.u.)[a]	Hydrogel	
	TiO_2-1	TiO_2-3
Before irradiation	2,442 ± 572	2,009 ± 327
After irradiation	2,387 ± 194	2,246 ± 116

[a] Spectra were collected with Hitachi F-4500 spectrophotometer at excitation/emission slits of 10/5 nm

The photosensitive properties of both the TiO_2 matrix and the immobilized porphyrin were examined with the use of the following experiments. In the first case, u.v. irradiation of both gel components for 1 h resulted in only slight changes in the region of both TPPS and TiO_2 absorption/emission spectra. The fluorescence intensities of TPPS after u.v. incidence are shown in Table 3. The data proved the photolytic stability and high biocompatibility of TiO_2. Furthermore, they also indicated the failure of TiO_2 to generate ROS, which manifested itself in the stability of

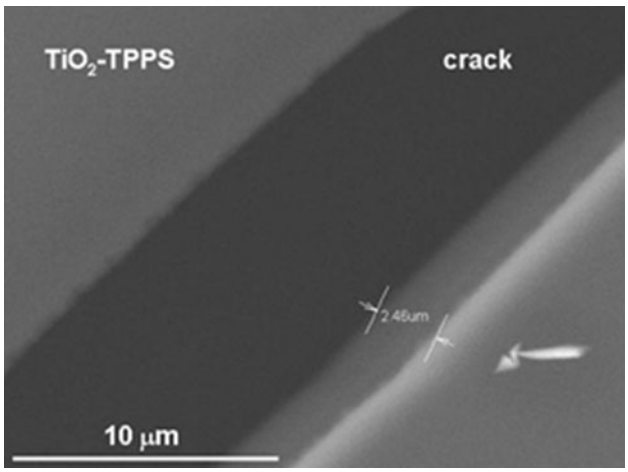

Fig. 5 SEM micrograph of TiO_2–TPPS

TPPS in the matrix. A similar situation was also observed with the immobilized TPPS that absorbed in the visible region.

It is worth noting that both indirect measurements of the surface ROS based on the light-induced production of I_3^- (for procedure see Sect. 2.6) and the direct measurement of $^1O_2$ lifetime inside the matrix at 1,270 nm after laser excitation of the porphyrin showed that the TiO_2–TPPS composites did not possess any photoactivity. It seems likely that the failure of the immobilized porphyrin to generate $^1O_2$ was due to the compact non-porous structure of the matrix (Fig. 5).

3.3 Controlled release of TPPS from the TiO_2 hydrogels

In spite of the stability of the composite layers in water, they were dissolved in biological buffers—citrate (100 mmol L^{-1})–phosphate(100 mmol L^{-1}; pH 6.0) and lactate (100 mmol L^{-1}; pH 5.5)—due to formation of the chelates with titanium(IV) species that led to the release of TPPS. The time dependence of TPPS dissolution upon the action of the chelating agents was determined by the absorption spectroscopy and smoothed by the Bolzmann sigmoid curves using the Origin software (Fig. 6). The curve parameters are shown in Table 4.

The hydrogels (TiO_2-1 and TiO_2-3) released TPPS faster in the citrate buffer, which was stronger chelating than the lactate. The rate of TPPS release from TiO_2-1 and TiO_2-3 measured in the exponential phase was 350 and 278 pmol min^{-1} in the lactate buffer, and 596 and 1,030 pmol min^{-1} in the citrate, resp. The observed faster TiO_2-3 dissolution in both chelating agents was due to the lower stability of the matrix containing the greater TEA/TiO_2 mol. ratio. In the lactate buffer, TiO_2-1 and TiO_2-3 dissolutions were complete in 80 and 96 min, respectively, while in the citrate buffer, TiO_2-3 was dissolved in 38 min and TiO_2-1 in 66 min.

3.4 Antimicrobial effect of TPPS released from TiO_2 hydrogels

The antimicrobial test with chemically triggered TPPS release was carried out by dissolving the porphyrin hydrogels in the sterile citrate–phosphate buffer exposed to sun light for 8 summer days by open window (see Sect. 2.8; Table 2). Although an unknown microbial culture was found in (6.41 ± 4.66) × 10^6 c.f.u. mL^{-1} concentration in the blank sample after 5 days, no contamination was observed with the buffer-released porphyrin hydrogels and the free TPPS during the whole experiment).

The same buffer inoculated with the model microorganism, *A. niger* 4054 strain, i.e. the mold resistant to citric acid, was poured onto the porphyrin hydrogels and illuminated with a halogen lamp (10 klx) for 48 h (see Sect. 2.8; Table 2). The highest photosterile effect was found for the free TPPS (Fig. 7). In its presence, the inactivation of the mold at the initial concentration of 2,200 c.f.u. mL^{-1} was complete after 24-h illumination

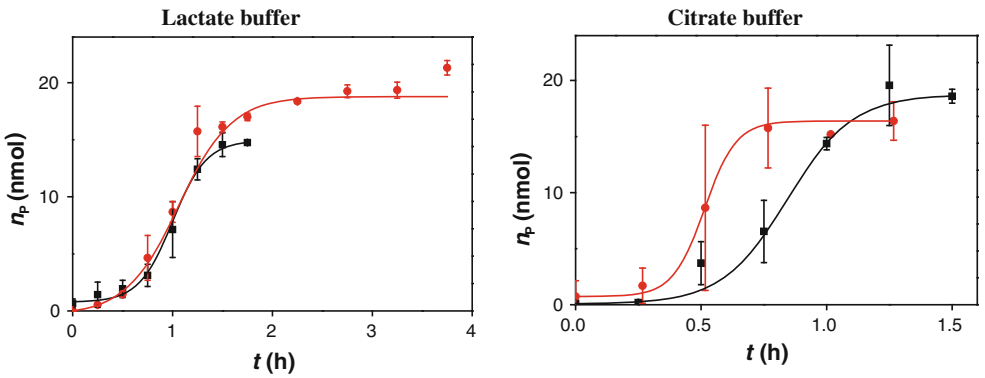

Fig. 6 TPPS release from TiO_2 hydrogels to 3 mL of the lactate (100 mmol L^{-1}; pH 5.5) and citrate (100 mmol L^{-1})–phosphate (100 mmol L^{-1}; pH 6.0) buffer at 200 rpm. *filled square* TiO_2-1, *filled circle* TiO_2-3

Table 4 Constants of the sigmoid Bolzmann curves fitting the kinetics of TPPS leaching from TiO_2 hydrogels in biological buffers

Constants	Lactate buffer		Citrate buffer	
	TiO_2-1	TiO_2-3	TiO_2-1	TiO_2-3
n_1[a]	0.76598	−0.33205	0.06614	0.73461
n_2[b]	14.9260	18.7784	18.7307	16.3824
t_c[c]	1.00073	1.06257	0.84362	0.51357
dt[d]	0.16883	0.02973	0.13038	0.06333
R^2	0.99893	0.99756	0.99720	0

[a] The lower limit of the curve

[b] The upper limit of the curve (a final molar amount of the leached TPPS)

[c] The inflex point of the exponential part of the curve corresponding to the time at the molar amount of $(n_1 + n_2)/2$

[d] The quarter time of the exponential part of the curve

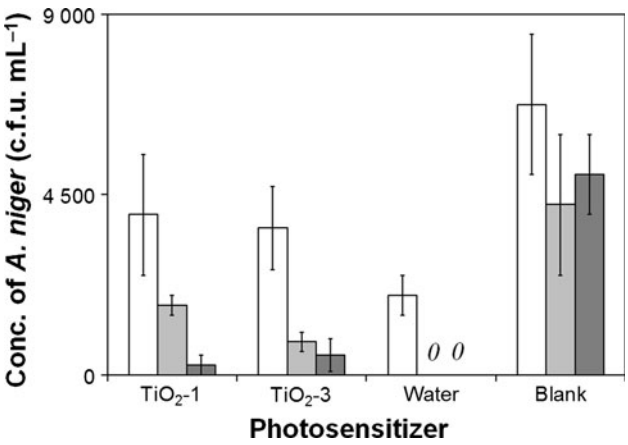

Fig. 7 Antimicrobial effect of TiO_2-1, TiO_2-3 and aqueous TPPS (4.8 μmol L^{-1}) in citrate (10 mmol L^{-1})–phosphate (20 mmol L^{-1}; pH 6.0) buffer against *A. niger* 4054 after illumination by a halogen lamp (10 klx). *White bar* Non-illuminated samples (0 J cm^{-2}), *gray bar* samples illuminated for 24 h (126 J cm^{-2}), and *black bar* 48 h (252 J cm^{-2})

(126 J cm^{-2}). The buffers with the dissolved TiO_2-1 and TiO_2-3 hydrogels showed biocidal effect, too. In these cases, the mould concentration decreased from 4,000 to 250 c.f.u. mL^{-1} and from 3,667 to 500 c.f.u. mL^{-1}, respectively. At the end of the experiment, the surface of the citrate buffer itself (blank sample) was covered by a film of mold.

4 Conclusion

Anionic TPPS photosensitizer has been immobilized into the titanium hydrogels stabilized by positively charged triethanolamine. Bonding ionic interactions and the lower polarity of the matrix compared to water led to changes in the absorption properties of the immobilized dye. The TiO_2 gels containing the entrapped TPPS were stable in water and highly biocompatible, not producing ROS after illumination with both u.v. and visible light. The presence of chelating agents (lactate and citrate) led to dissolution of the titanium matrix and the controlled TPPS release. The rate of the dissolution depended on the TEA concentration in the matrix and on the buffer, the citrate being the more effective than the lactate. After illumination with a halogen lamp, the released dye was effective against *A. niger* 4054 strain as a model microorganism. Exposure of the sterile phosphate–citrate buffer to day light prolonged its sterility.

The titanium materials under study may be prospective materials for treatment of infections.

Acknowledgments This work was supported by the Ministry of Education, Youth and Sports of the Czech Republic, ME892 grant. The authors express their gratitude to the Swedish Research Council (Vetenskapsrådet) for the support of the project "Molecular Precursors and Molecular Models of Nanoporous Materials".

References

1. Jori G, Camerin M, Soncin M, Guidolin L, Coppellotti O (2011) In: Hamblin MR, Jori G (eds) Photodynamic inactivation of microbial pathogens: medical and environmental application. Book series: comprehensive series in photochemistry and photobiology-series 11:1–18
2. Rychtáriková R, Kuncová G (2009) Immobilized singlet oxygen photosensitizers and their antimicrobial effect. Chem Listy 103:800–813
3. Caminos DA, Spesia MB, Pons P, Durantini EN (2008) Mechanisms of *Escherichia coli* photodynamic inactivation by an amphiphilic tricationic porphyrin and 5,10,15,20-tetra(*N*,*N*,*N*-trimethylammoniumphenyl)porphyrin. Photochem Photobiol Sci 7:1071–1078
4. Jori G, Fabris C, Soncin M, Ferro S, Coppellotti O, Dei D, Fantetti L, Chiti G, Roncucci G (2006) Photodynamic therapy in the treatment of microbial infections: basic principles and perspective applications. Laser Surg Med 38:468–481
5. Lukšienė Ž (2005) New approach to inactivation of harmful and pathogenic microorganisms by photosensitization. Food Technol Biotechnol 43:411–418
6. Hegge B, Andersen T, Melvik JE, Kristensen S, Tonnesen HH (2010) Evaluation of novel alginate foams as drug delivery systems in antimicrobial photodynamic therapy (aPDT) of infected

wounds—an in vitro study: studies on curcumin and curcuminoides XL. J Pharm Sci 99:3499–3513
7. Jones DS, Lorimer CJ, Andrews GP, McCoy CP, Gorman SP (2007) An examination of the thermorheological and drug release properties of zinc tetraphenylporphyrin-containing thermoresponsive hydrogels, designed as light activated antimicrobial implants. Chem Eng Sci 62:990–999
8. Donnelly RF, McCarron PA, Lightowler JM, Woolfson AD (2005) Bioadhesive patch-based delivery of 5-aminolevulinic acid to the nail for photodynamic therapy of onychomycosis. J Control Release 103:381–392
9. Donnelly RF, McCarron PA, Tunney MM, Woolfson AD (2007) Potential of photodynamic therapy in treatment of fungal infections of the mouth. Design and characterisation of a mucoadhesive patch containing toluidine blue O. J Photochem Photobiol B Biol 86:59–69
10. Donnelly RF, Cassidy CM, Loughlin RG, Brown A, Tunney MM, Jenkins MG, McCarron PA (2009) Delivery of methylene blue and meso-tetra(N-methyl-4-pyridyl)porphine tetratosylate from cross-linked poly(vinyl alcohol) hydrogels: a potential means of photodynamic therapy of infected wounds. J Photochem Photobiol B Biol 96:223–231
11. Arruebo M (2012) Drug delivery from structured porous inorganic materials. WIREs Nanomed Nanobiotechnol 4:16–30
12. Chiriac AP, Neamtu I, Nita LE, Nistor MT (2010) Sol gel method performed for biomedical products implementation. Mini-Rev Med Chem 10:990–1013
13. Menaa B, Menaa F, Aiolfi-Guimaraes C, Sharts O (2010) Silica-based nanoporous sol–gel glasses: from bioencapsulation to protein folding studies. Int J Nanotechnol 7:1–45
14. Fujiwara M, Shiokawa K, Morigaki K, Zhu YC, Nakahara Y (2008) Calcium carbonate microcapsules encapsulating biomacromolecules. Chem Eng J 137:14–22
15. Seisenbaeva GA, Moloney MP, Tekoriute R, Hardy-Dessource A, Nedelec J-M, Gun'ko YK, Kessler VG (2010) Nanostructured metal oxide microparticles; potential scaffolds for drug delivery and catalysis. Langmuir 26:9809–9817
16. Kessler VG, Seisenbaeva GA, Unell M, Håkansson S (2008) Chemically triggered biodelivery using metal–organic sol–gel synthesis. Angew Chem 120:8634–8637
17. Crawford GA, Chawla N, Das K, Bose S, Bandyopadhyay A (2007) Microstructure and deformation behavior of biocompatible TiO_2 nanotubes on titanium substrate. Acta Biomater 3:359–367
18. Livage J, Coradin T (2005) In: Kozuka H (ed) Handbook of sol–gel science and technology: processing characterization and applications, vol 1. Kluwer, Norwell
19. Kessler VG, Seisenbaeva GA, Håkansson S (2007) Metal oxide hydrogels and hydrosols, their preparation and use. WIPO Pat. Application, WO/2007/145573A1
20. Mosinger J, Mosinger B (1995) Photodynamic sensitizers assay: rapid and sensitive iodometric measurement. Experientia 51:106–109
21. Kessler VG (2009) The chemistry behind the sol–gel synthesis of complex oxide nanoparticles for bio-imaging applications. J Sol–Gel Sci Technol 51:264–271
22. Ou Z, Yao H, Kimura K (2007) Preparation and optical properties of organic nanoparticles of porphyrins without self-aggregation. J Photochem Photobiol A Chem 189:7–14
23. Yoshida A, Kakegawa N, Ogawa M (2003) Adsorption of a cationic porphyrin onto mesoporous silicas. Res Chem Intermed 29:721–731
24. Matthews RW, McEvoy SR (1992) A comparison of 254 nm and 350 nm excitation of TiO_2 in simple photocatalytic reactors. J Photochem Photobiol A Chem 66:355–366
25. Yang H, Zhu S, Ning P (2004) Studying the mechanisms of titanium dioxide as ultraviolet-blocking additive for films and fabrics by an improved scheme. J Appl Polym Sci 92:3201–3210